La mer 42 : 21–34, 2004
Sociêté franco-japonaise d'océanographie, Tokyo

Direct Current Measurements with special reference to Velocity Fields of Mesoscale Eddies in the Shikoku Basin

Yoshihiko SEKINE[*1] and Toshiyuki MASUZAWA[*2]

Abstract : We have made two direct current measurements at 29.50°N and 135.25°E in the Shikoku Basin over the periods from 20 February to 16 April in 1999 at a depth of 470 m and from 17 April to 9 December in 1999 at a depth of 730 m. Main results of these direct current measurements are presented in this paper. It is shown that variations in the velocity is essentially due to the inertial oscillation with a period of a day. It is also shown that the inertial oscillation is added over the mean flow of mesoscale eddies estimated from the sea surface height observed by the TOPEX/POSEIDON pass the observational station and it commonly coincides with the deepening of the current meter by the larger dragging effect of the larger horizontal velocity. The mesoscale eddies have a horizontal velocity of about 15 cm sec^{-1} in a middle layer with a depth of 500–700 m, which indicates the mesoscale eddies detected from the satellite altimeter have a vertical structure and it has a possibility to give a dynamical influence on the path dynamics of the Kuroshio.

Keywords : *Inertial oscillation, mesoscale eddy, direct current measurement*

1. Introduction

Recently, some long-term direct current measurements have been carried out (e.g., FUJIO *et al.,* 2000; IMAWAKI *et al.,* 2001) and various velocity variations are detected. In particular, general deep layer circulation in the Shikoku Basin has been observed by some direct current measurements (TAIRA and TERAMOTO, 1981, 1985; NISHIDA and KURAMOTO, 1982; ISHIZAKI *et al.,* 1983; FUKASAWA *et al.,* 1986; TAIRA *et al.,* 1990). On the other hand, influence of mesoscale eddies on the path variation of the Kuroshio has been discussed by some authors (YOSHIKAWA *et al.,* 1998; ICHIKAWA, 2001; EBUCHI and HANAWA, 2003). It is commonly pointed out that the anticyclonic eddy formed in the Kuroshio Extension propagated southwestward and collided with the main Kuroshio flow in the south of Kyushu, and triggered a small meander off Kyushu. Furthermore, EBUCHI and HANAWA (2003) showed that the cyclonic eddy propagated to the south of Shikoku and collided with the Kuroshio to form a small meander path of the Kuroshio.

Several numerical experiments have been performed to see the dynamical effect of an anticyclonic eddy inserted artificially in ocean models on the Kuroshio path variation (AKITOMO and KUROGI, 2001; MITSUDERA *et al.,* 2001; ENDOH and HIBIYA, 2001). They commonly showed that the anticyclonic eddy given in the numerical model yields a meander path of the Kuroshio.

Here, we should notice that the mesoscale eddies discussed in these studies are essentially detected from the sea surface height estimated by the satellite observation of TOPEX/POSEIDON (e.g., KURAGANO and KAMACHI, 2000), the vertical velocity structure of mesoscale eddies has not been well observed by

[*1] Institute of Physical Oceanography and Climate, Faculty of Bioresources, Mie University, Tsu 514-8507, Japan
[*2] Department of Hydrospheric-Atmospheric Science, Graduate School of Environmental Studies, Nagoya University, Nagoya 464-8601, Japan
[*] Corresponding author, E-mail:sekine@bio.mie-u.ac.jp

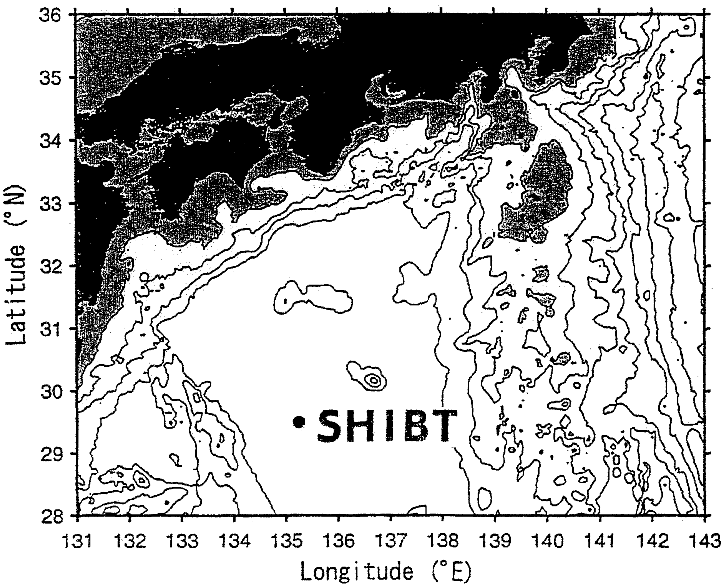

Fig. 1 Location of the station (SHIBT) of the direct current measurements of the present study. Isopleth of depth with a contour interval of 1000 m is also shown and the regions with the depth shallower than 1000 m are stippled.

direct current measurements. Therefore, the assumption of the vertical structure of the mesoscale eddies inserted in the numerical model should be checked by use of the observational data.

In order to see this problems, we have made a direct current measurements at Station SHIBT (**SHI**ikoku **B**asin **T**ime series; 135.25°E, 29.50°N) in the Shikoku Basin shown in Fig. 1 (LI *et al.*, 2004). The observational station is in the interior region where mesoscale eddies have a tendency to pass over this latitudes (MITUDERA *et al.*, 2001; EBUCHI and HANAWA, 2003). Even though a small meander of the Kuroshio off Kyushu is generated, the path of the small meander can not develop to the observational point. The first observation was made over the periods from 20 February to 16 April 1999 and the current meter is set at a depth of 470 m. The second observation was made from 17 April to 9 December 1999 at a depth of 730 m.

The main results of the current observation is presented in this paper. In the following, details of the observation will be mentioned in the next section. Results of the direct current measurements will be noted in the section 3. Summary and discussion will be made in section 4.

2. Observations

Direct current measurements were made by use of a doppler current meter (AANDERAA RCM-9) deployed at 20 m above the upper sediment trap of a sediment trap mooring system at 500 m and 4000 m (LI *et al.*, 2004). The first mooring system with the current meter at a depth of 470 m at 135.251°E and 29.507°N with a ocean depth of 4511 m was set on 20 February 1999 by Research Vessel "Yokosuka" of JAMSTEC and was recovered on 16 April 1999 by use of the Training Vessel "Seisui-maru" of Mie University. The observed velocity data at every 30 minutes in this period is hereafter referred to as the first mooring case.

The second mooring system with a current meter at a depth of 730 m at 135.234°E and 29.473°N with a ocean depth of 4610 m was set on 17 April 1999 by use of "Seisui-maru" and recovered on 9 December 1999 by use of the Research Vessel "Tansei-maru" of Ocean Research Institute of University of Tokyo, of which observed velocity data at every 60 minutes is referred to as the second mooring case. The difference in the current meter depth

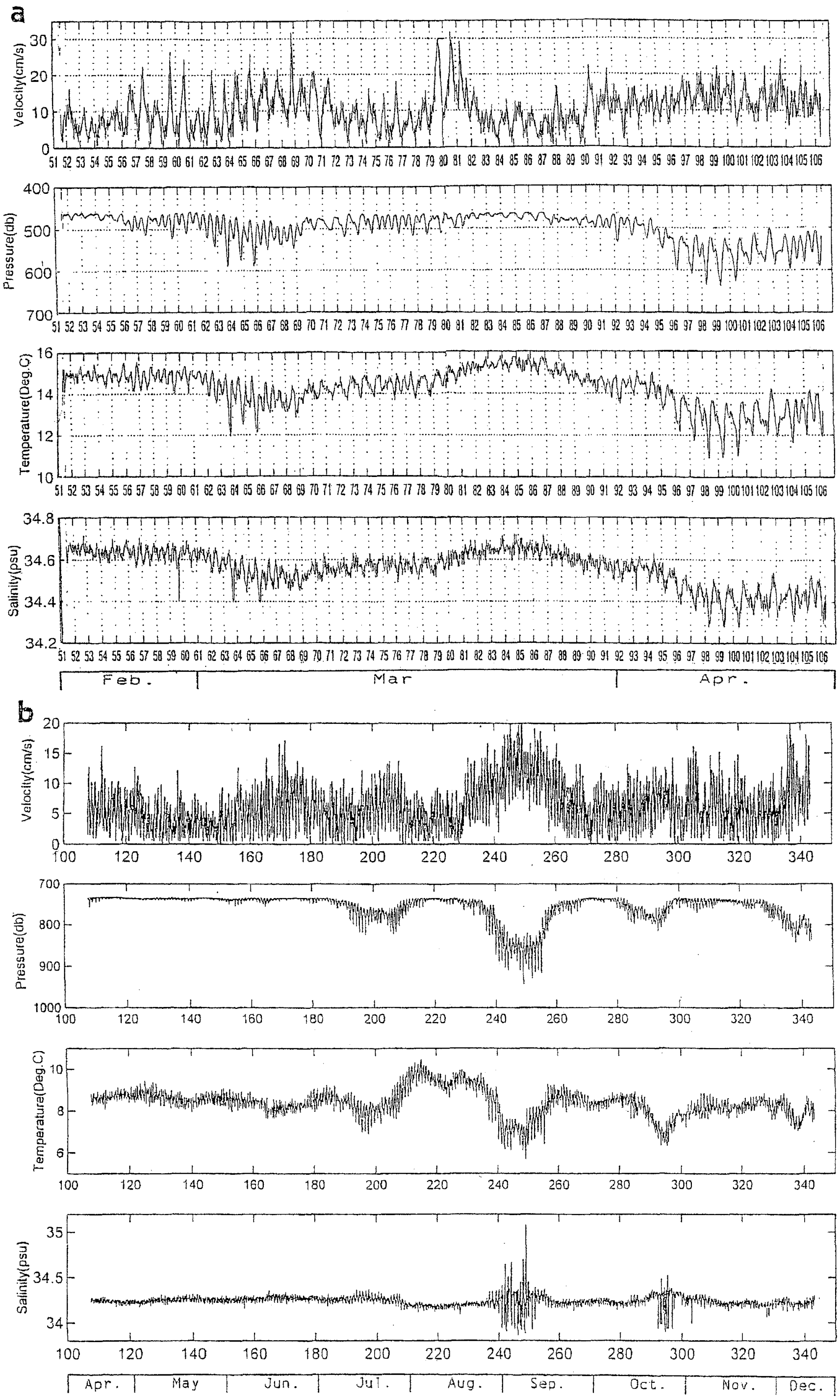

Fig. 2 Time variation in the observed current speed (absolute velocity) (top), pressure (upper middle) temperature (lower middle) and salinity (bottom), during (a) first mooring case and (b) second mooring case. Numbers along the axis of abscissas are days from a new year (Julian days).

between the two mooring cases was due to that of sea floor depth and to intertwining of mooring ropes during the second mooring case. Type of the sinker and the buoyancy force of the mooring system by use of the sixteen buoys are same in both the observations, in which the weight of sinker is 650 kg (565 kg in situ)and the actual buoyancy force of the buoys is 140 kg.

3. Observational results

In order to see the observational condition of the mooring system, the observed pressure of the current meter is shown in Fig. 2 together with the observed absolute velocity, temperature and salinity. In the first mooring case (Fig. 2a), semidiurnal variation of the pressure is observed in early March, while the semidiurnal variation is relatively weak in last 10 days in March. Two periods of increase in the pressure are observed in early March and in April. Periodic vertical change of the pressure is observed in early March and the amplitude of the pressure variation exceeds 100 db, in which the current meter moves in the depth range from 470 m to 580 m. A long period downward shift of the current meter with a diurnal variation is observed in April. As the salinity minimum layer formed by the North Pacific Intermediate Water exists in the depths of 800 m in this region (e.g., SEKINE, 2002a), low temperature and low salinity are essentially observed when the current meter shifts to a deeper level in the first mooring case. As the current meter shifts to a deeper level than 800 m, salinity is slightly increased in the second mooring case, whereas some noises are also observed.

More prominent downward shift of the current meter is seen in the second mooring case (Fig. 2b). Here, please notice that the scales of the ordinates and abscissas of Fig. 2b is different from those of Fig. 2a. During early September, the current meter moves in the depth range from 720 m to 910 m. Other two downward shifts of the current meter are detected in middle July and October and low temperature and high salinity are observed in these periods. Another prominent downward shift of the current meter is seen in the last period of the observation, complete observational data during the downward shift have not been obtained.

It should be noted that a larger absolute velocity is commonly observed in the periods with the downward shift of the current meter. It is suggested that the larger velocity induces a large horizontal drawing force on the mooring system and it forces the mooring system to shift to the downstream area. Since the length of the mooring system from the sinker to the current meter is constant, the large horizontal drawing force induces the downward shift of the current meter.

We should correct the observational data by the influence of downward shift of the current meter. However, because the vertical velocity difference estimated from the geostrophic flow estimation is not so large in the depth range with the vertical shift of the current meter (SEKINE, 2002b)and because we will not discuss the temperature, salinity and velocity variation at a fixed depth in this range, the revision of the observational data by the vertical shift of the current meter is not carried out.

Stick diagrams of the observed velocities at every 30 minutes (60 minutes)observed by the first and second mooring cases are shown in Fig. 3 (Fig. 4). In general, velocity oscillation with a period of one day essentially dominated. However, some periods with almost uniform larger velocities are also detected and a mechanical velocity variation is inferred.

To see the velocity variations more quantitatively, rotary spectrum of the observed velocity is shown in Fig. 5. In both cases, a prominent peak is found in a period of 24 hours. Another peak with a period of 12 hours is also commonly seen, however there exist no other common peaks between the two mooring cases. Rotary coefficient of the rotary spectrum is shown in Fig. 6. For both cases, positive coefficient showing the anticyclonic (clockwise) circulation is significantly large for the peak with periods of 24 hours and 12 hours. Velocity variations with the period of 24 hours is caused by the inertial oscillation induced by the Coriolis force with the period of a day (T); $2\pi/f = T/(2\sin(\phi)) \sim T$, where f and ϕ are the Coriolis parameter and the latitude of 29.50° in this case. The velocity variations with the period of 12 hours are due to the tidal flow

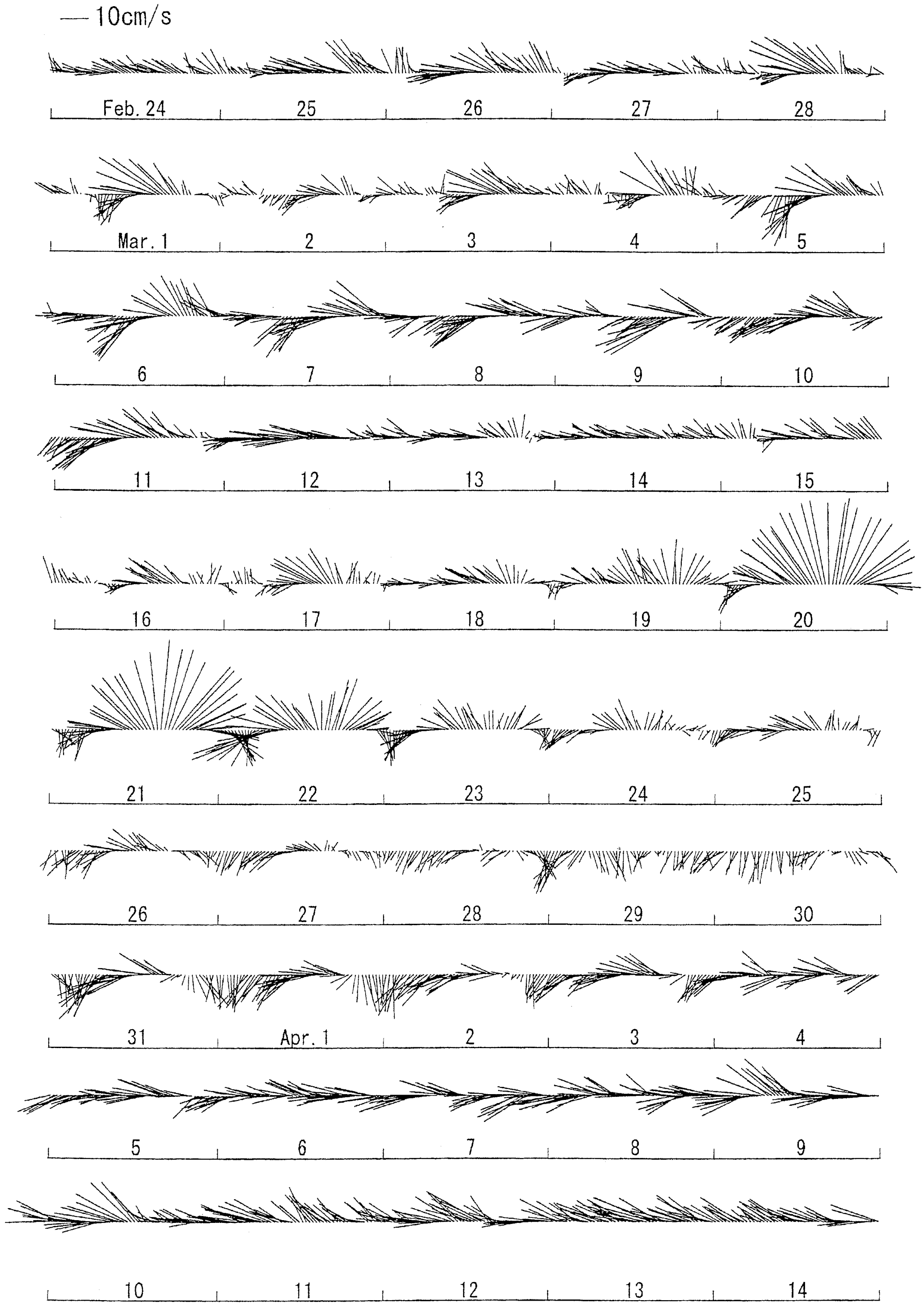

Fig. 3 Northward stick diagram of the observed velocity vectors in the first mooring case.

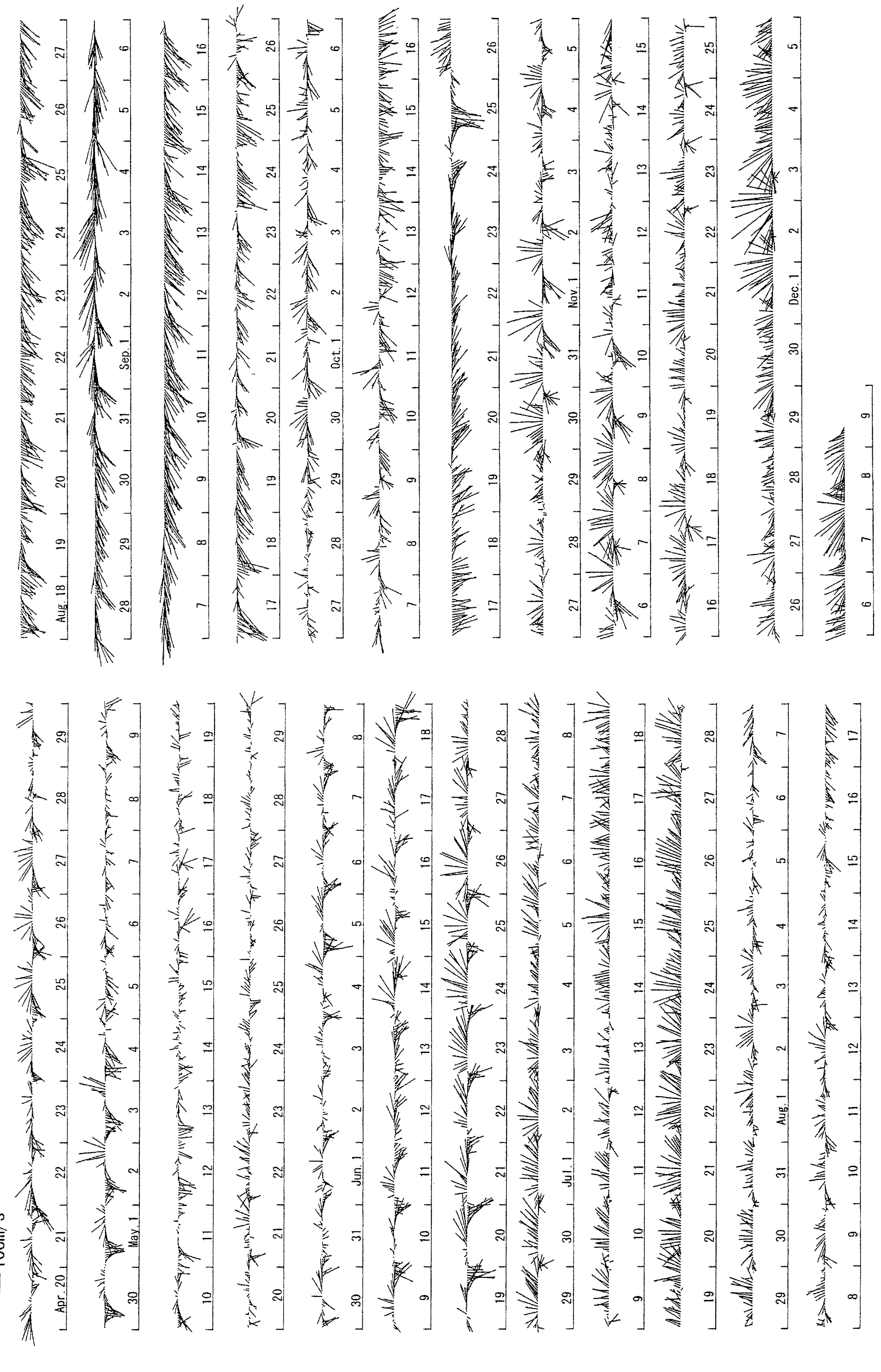

Fig. 4 Northward stick diagram of the observed velocity vectors in the second mooring case.

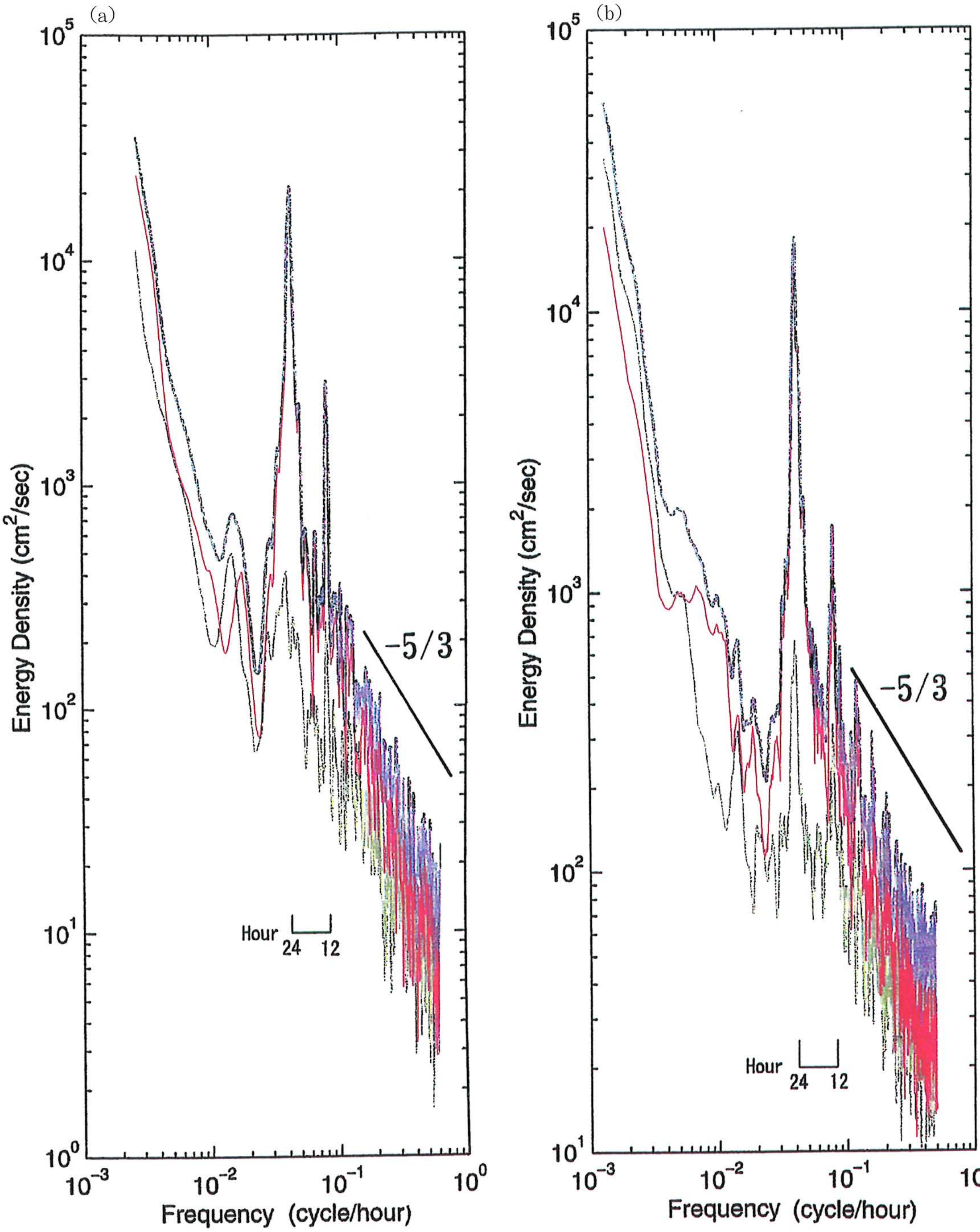

Fig. 5 Rotary spectrum of the observed velocity. (a) First mooring case and (b) second mooring case. Blue lines show the total spectrum, red (green) line represents the anticyclonic clockwise (cyclonic counterclockwise) circulation.

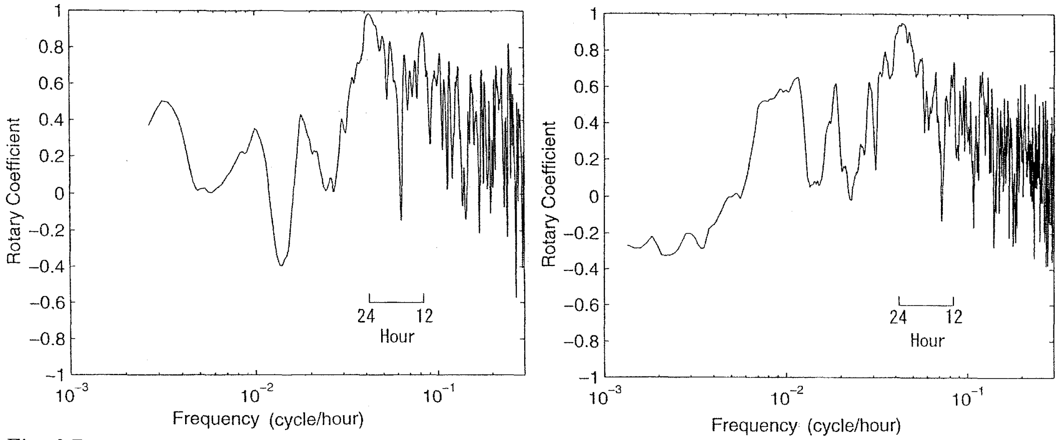

Fig. 6 Rotary coefficient of the rotary spectrum. First mooring case (left panel) and the second mooring case (right panel).

oscillation. Detailed analyses on the diurnal variations including the inertial oscillation, K_1 with the period of 23.93 hours and O_1 with 25.82 hours, and on the half diurnal variations including M_2 (12.42 hours) and S_2 (12.00 hours) seem to be possible by use of the long-term observational data. However, because FFT analyses by use of hourly data yield some inevitable error, results of the detailed analyses are not shown.

Mean slope (gradient) of the rotary spectrum (Fig. 5) in the shorter periods between 10 hours and 4 hours is −2.1 for the first mooring case and −2.3 for the second mooring case. These slopes are larger than the −5/3 power law of the Kolmogorov Spectrum (OZMIDOV, 1965) and relatively well approximated by the −2 power law of the GARRETT and MUNK Spectrum (GARRETT and MUNK, 1971, 1975), which indicates that the short period velocity variation is mainly due to internal waves. However, the slope of the spectrum is decreased if the estimated range is shifted to shorter period. Therefore, the slope of the spectrum has a tendency to represent the inertial subrange of the −5/3 power law of the Kolmogorov Spectrum in more shorter periods.

Based on the dominant inertial oscillation shown by the rotary spectrum (Fig. 5), progressive velocity vector diagram of the second mooring case is shown in Fig. 7. It is clearly seen that the clockwise inertial oscillation with a period of 24 hours is dominant in the observed velocity fields. Here, it should be noticed from Fig. 7a that the inertial oscillation is relatively weak and it is not clearly seen in some time periods; from 190 days to 210 days, 240 days to 260 days, 280 days to 300 days and 320 days to 340 days, while a large horizontal shift is commonly detected in these periods. In these periods, northward progress, southwestward progress, a cyclonic southward progress and northwestward progress are suggested from Fig. 7a, respectively. Mean velocities during these periods are 5.8 cm sec^{-1} 11.4 cm sec^{-1}, 6.3 cm sec^{-1} and 6.2 cm sec^{-1}. These periods commonly correspond to the downward shift of the current meter shown in Fig. 2b. The power spectrum during the large horizontal shift is shown in Fig. 8. Here, period of 5.3 days during the large velocity with coherent direction is adopted from Fig. 4. It is shown from Fig. 8 that the peak of 24 hours are still clear, while its intensity is not so clear as that in total period shown in Fig. 5. The constant of the FFT analysies of these case is large in comparison with the total period shown in Fig. 5. Therefore, the inertial oscillation with the bias of the mean flow is suggested in these periods.

In order to see the oceanic condition of the larger velocity periods accompanied by the downward shift of the current meter, sea surface velocity estimated from the sea surface height observed by the satellite observation of TOPEX/POSEIDON (KURAGANO and KAMACHI, 2000)is shown in Fig. 9. Together

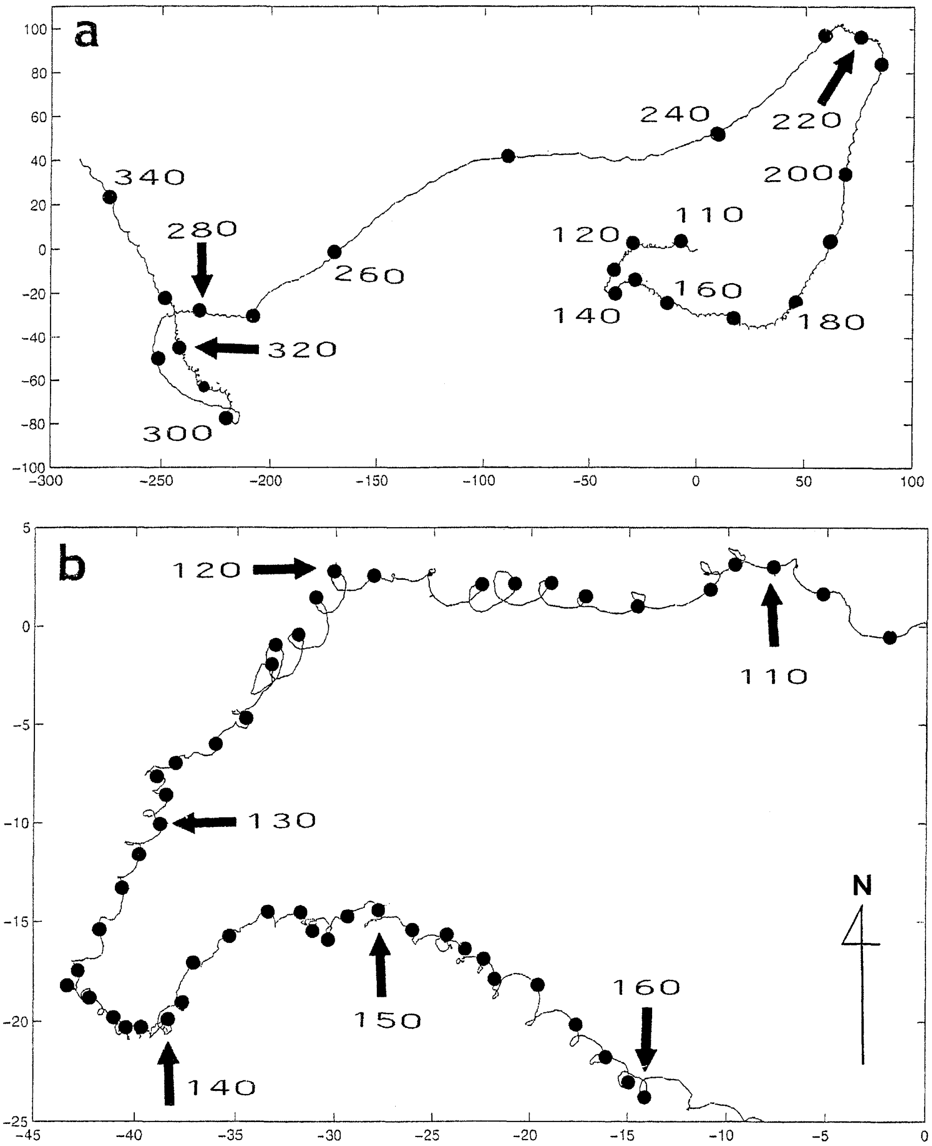

Fig. 7 (a) Progressive velocity vector diagram in the second mooring system. (b) Enlargement of the period from the initial stage to 160 Julian days. Numbers show the Julian days as were shown in Fig. 2b.

with Figs. 4 and 7a, it is found that the northeastward flow during the period of 190 days to 210 days is caused by the approach of the anticyclonic eddy with the northeastward flow in its western part (Fig. 9a). During the period of 240 days to 260 days, the southwestward flow is also suggested by the approach of the anticyclonic eddy and cyclonic eddy (Fig. 9b). Southward flow from 280 days to 300 days and northwestward flow from 320 days to 340 days are also explained by the coupled anticyclonic eddy and cyclonic eddy (Fig. 9c) and approach of the anticyclonic eddy (Fig. 9d), respectively. As for the downward shift of the current meter in early April in the first mooring case (Fig. 2a) with larger westward flow (Fig. 3), the approach of a cyclonic eddy south of the observational point and an anticyclonic eddy in

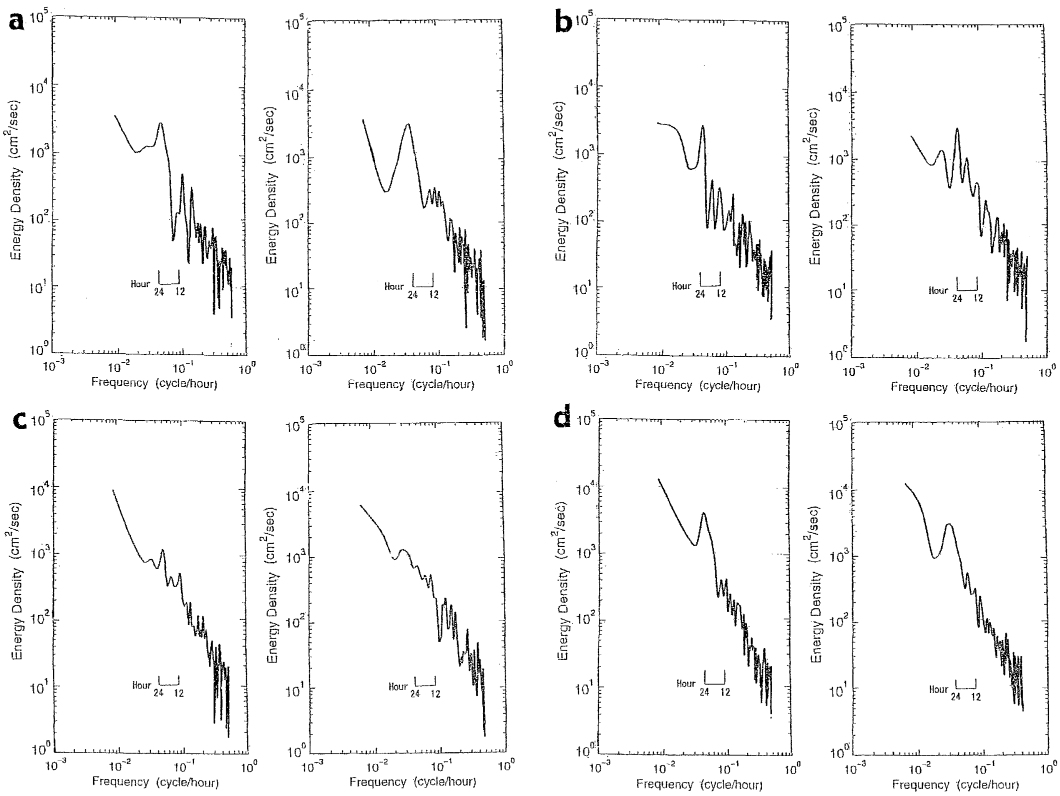

Fig. 8 Power spectrum in the periods of large horizontal shites with coherent direction during 5.3 days from (a) 21 July, (b) 13 September, (c) 13 October and (d) 2 December. The left (right) panel shows the power spectrum of eastward (northward) velocity.

northern region are seen in the surface velocity fields shown in Fig. 10.

Since mean velocities of the westward shift of the mesoscale eddies are about 6.8 cm sec^{-1} (EBUCHI and HANAWA, 2000), the monthly westward shift of a mesoscale eddy are about 180 km, which is not so fast and the almost uniform velocity has a possibility to be maintained in a horizontal distance shown in Fig. 7. It is thus resulted that mesoscale eddies have a vertical structure deeper than 700 m with a mean velocity of 15 cm sec^{-1}. Together with larger surface velocity shown in Figs. 9 and 10, a possible dynamical influence of mesoscale eddies on the path dynamics of the Kuroshio is suggested.

4. Summary and discussion

We have made two direct current measurements at 29.50°N and 135.25°E in the Shikoku Basin (Fig. 1)over the periods from 20 February to 16 April in 1999 at a depth of 470 m and from 17 April to 9 December in 1999 at a depth of 730 m. Main results of these direct current measurements are summarized as follows.

(1) Inertial velocity oscillation with a period of one day is dominated in the velocity variation and the clockwise circulation is seen in the progressive velocity vector diagram. However, some periods of large uniform velocity are also observed and the inertial oscillation is added over the bias of uniform velocity in this period.

(2) During the periods of some almost uniform velocities, downward shift of the current meter and the large velocity are commonly observed. It is suggested that the larger uniform velocity yields a larger dragging force on the mooring system, which results in the downward shift of

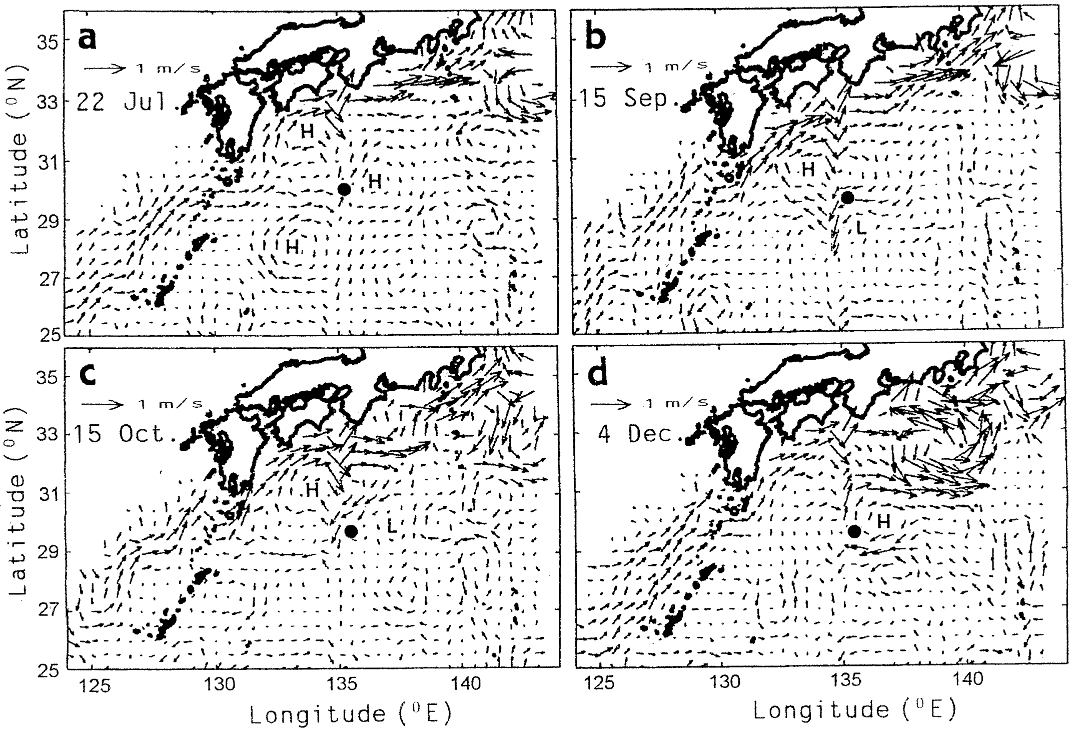

Fig. 9 Sea surface velocity estimated from the sea surface height observed by the satellite TOPEX/POSEIDON (KURAGANO and KAMACHI, 2000) during the second mooring case. Date of the observational and reference velocity are shown in left top of each panel. The observational point of the mooring system is also shown by closed circle.

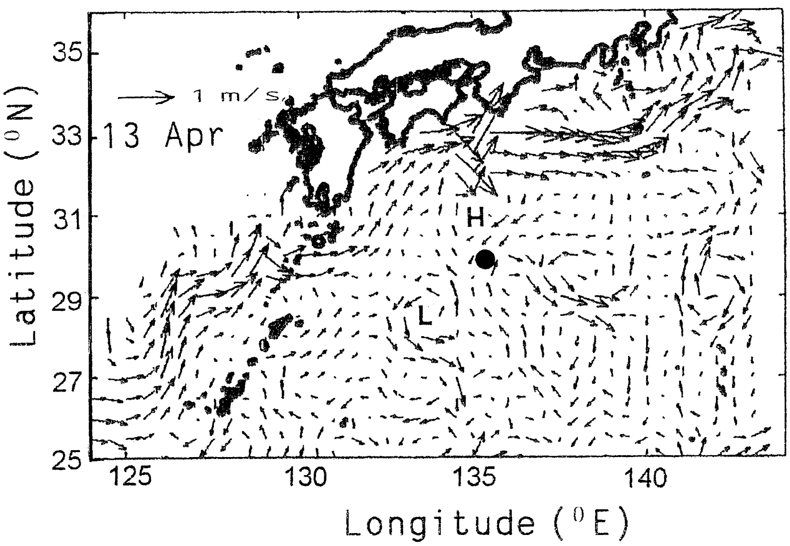

Fig. 10 Same as in Fig. 9, except for 13 April 1999 in period of the first mooring case.

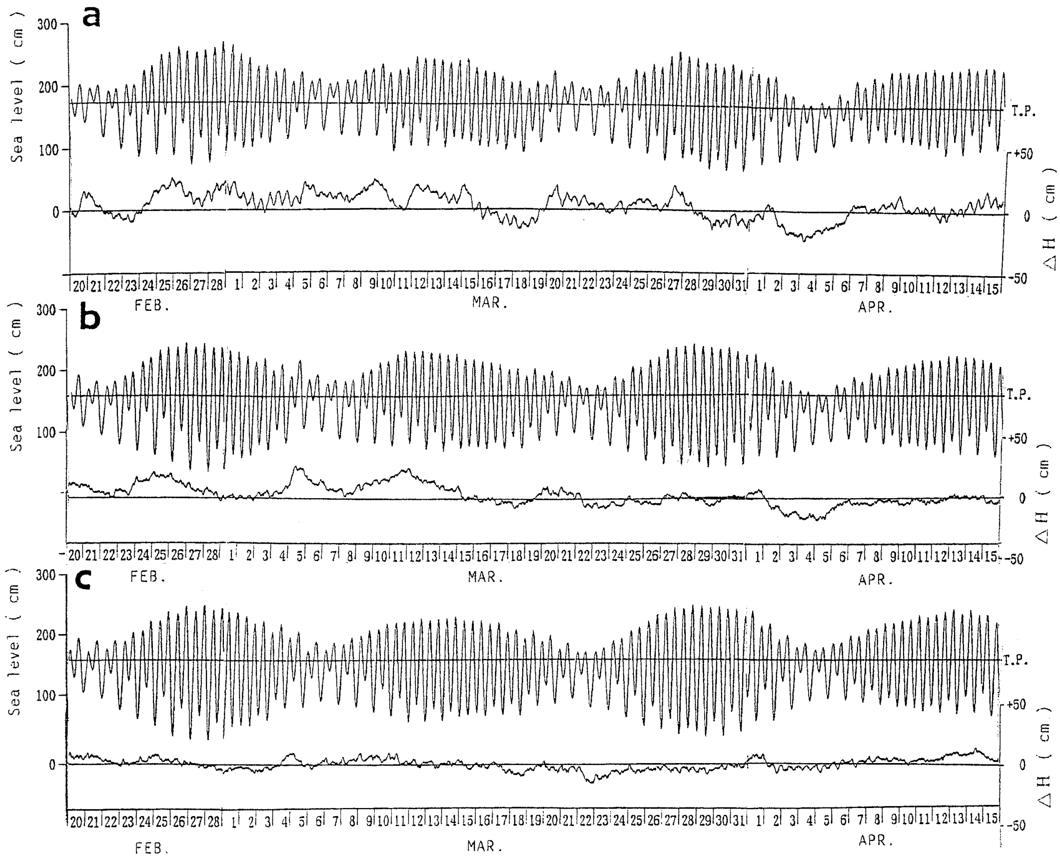

Fig. 11 Hourly sea level variation (upper)and their deviation from the predicted sea level (lower) based on the Climate and Marine Department of the Japan Meteorological Agency (1999). (a)Kushimoto, (b)Aburatsu and (c)Naha.

the current meter by the constraint of constant length of the mooring system from sinker to the current meter.
(3) The larger uniform velocity noted in (2) is caused by the approach of mesoscale eddies, which were detected by the satellite sea surface level. It is resulted that the mesoscale eddies have a vertical structure deeper than 700 m and a mean velocity of 15 cm sec^{-1} at an observed depth.

Larger velocity with an inertial oscillation is observed in 20–23 in March (Fig. 3), which is also shown by the large absolute velocity in Fig. 2. Because no significant atmospheric disturbance such as typhoon was observed in this observational period, it is inferred that the large inertial velocity may be related to the large sea level difference during the spring tide. So, the sea level variations at Kushimoto, Aburatsu and Naha are shown in Fig. 11. It is seen from Fig. 11 that the period of 20–23 in March is in the neap tide and the amplitude of the sea level variation is rather small. However, since the diurnal tide is essentially dominant in this period (Fig. 11), the resonant phenomenon between the tidal current and the inertial oscillation is suggested in this case. Similar large amplitude velocity oscillations in 23–25 June (Fig. 4), and 30–31 October are also observed in the neap tide with a diurnal tide variation (not shown). A resonant effect between the inertial oscillation and the diurnal tide is inferred, however its detailed dynamics will be left out for future study.

Acknowledgments

We would like to thank captains, officers and crews of the training vessel "Seisui-maru" of Mie University, Research Vessel "Yokosuka" of JAMSTEC and Research Vessel "Tansei-Maru" of Ocean Research Institute of University of Tokyo for their skillful assistance during the observations. The valuable comment of the reviewer is very helpful to revise the manuscript. The thanks are extended to the valuable comment on the dynamics of the tidal current by Profs. T. YANAGI of Kyushu University, H. TAKEOKA of Ehime University and T. HIBIYA of University of Tokyo. This work was supported in part by Special Research Project on Dynamics of Atmosphere-Ocean Interaction of Institute for Hydrospheric-Atmospheric Sciences Nagoya University.

References

AKITOMO, K. and M. KUROGI(2001): Path transition of the Kuroshio due to mesoscale eddies: a two-layer, wind-driven experiment. J. Oceanogr., **57**, 735-741.

Climate and Marine Department of Japan Meteorological Agency (1999): Monthly Mean Ocean Report Nos. 74-76.

EBUCHI, N. and K. HANAWA(2000): Mesoscale eddies observed by TOLEX-ADCP and TOPEX/POSEIDON altimeter in the Kuroshio recirculation region south of Japan. J. Oceanogr., **56**, 43-57.

EBUCHI, N. and K. HANAWA(2003): Influence of mesoscale eddies on variations of the Kuroshio path south of Japan. J. Oceanogr., **59**, 25-36.

ENDOH, T. and T. HIBIYA(2001): Numerical simulation of the transient response of the Kuroshio leading to the large meander formation south of Japan. J. Geophys. Res., **106**, 26833-26850.

FUJIO, S., D. YANAGHIMOTO and K. TAIRA(2000): Deep current above the Izu- Ogasawara Trench. J. Geophys. Res., **105**, 6377-6386.

FUKASAWA, M., T. TERAMOTO and K. TAIRA(1986): Abyssal current along the periphery of Shikoku Basin. J. Oceanogr. Soc., Japan, **42**, 459-472.

GARRET, C. and W.H. MUNK(1971): Internal wave spectra in the presence of finite structure. J. Phys. Oceanogr., **1**, 196-202.

GARRET, C. and W.H. MUNK(1975): Space-time scales of internal waves: a progress report. J. Geophys. Res., **80**, 196-297.

ICHIKAWA, K. (2001): Variation of the Kuroshio in the Tokara Strait induced by mesoscale eddies. J. Oceanogr., **57**, 55-68.

IMAWAKI, S., H. UCHIDA, H. ICHIKAWA, M. FUKASAWA, S. UMATANI and ASUKA group (2001): Satellite altimeter monitoring of the Kuroshio transport south of Japan. Geophys. Res. Lett., **28**, 17-20.

ISHIZAKI, H., O. ASAOKA, S. KONAGA and M. TAKAHASHI(1983): Direct measurement of near bottom current on the continental slope off Omaezaki, central Japan. Pap. Met. Geophys., **33**, 257-268.

KURAGANO, T., M. KAMACHI(2000): Global statistical space-time scales of oceanic variability estimation from the TOPEX/POSEIDON altimeter data. J. Geophys. Res., **105**, 955-974.

LI, T., T. MASUZAWA, H. KITAGAWA(2004): Seasonal variations in setting fluxes of major components in the oligotrophic Shikoku Basin, the western North Pacific: Coincidence of high biogenic flux with Asian dust supply in spring. Mar. Chem. (in press).

MITSUDERA, H., T. WASEDA and Y. YOSHIKAWA(2001): Anti-cyclonic eddies and Kuroshio meander formation. Geophys. Res. Lett., **28**, 2025-2028.

NISHIDA, H. and S. KURAMOTO(1982): Deep current of the Kuroshio around the Izu Ridge-Large meander of the Kuroshio in 1975-1980 (IV), Rept. Hydrogr. Res., Tokyo, No. **17**, 241-255.

OZMIDOV, R. V. (1965): Energy distribution between oceanic motions of different scales. Bull. Acad. Sci. U.S.S.R. Atmos. Oceanic Phys., **1**, 257-261.

SEKINE, Y. (2002a): Temperature and salinity distribution across the Kuroshio in the Shikoku Basin. Bull. Fac. Biores. Mie Univ., No. **29**, 63-74.

SEKINE, Y. (2002b): Geostrophic velocity of the Kuroshio south of Japan. Bull. Fac. Biores. Mie Univ., No. **29**, 75-86.

TAIRA, K. and T. TERAMOTO(1981): Velocity fluctuations of the Kuroshio near the Izu Ridge and their relationship to current path. Deep-Sea Res., **28**, 1187-1197.

TAIRA, K. and T. TERAMOTO (1985): Bottom current in Nankai Trough and Sagami Trough. J. Oceanogr. Soc. Japan, **41**, 388-398.

TAIRA, K., S. KITAGAWA, K. UEHARA, H. ICHIKAWA, H. HACHIYA and T. TERAMOTO (1990): Direct measurements of mid-depth circulation in the Shikoku Basin by tracking SOFAR floats. J. Oceanogr. Soc. Japan, **46**, 296-306.

YOSHIKAWA, Y., M.-S. KIM and H. MITSUDERA(1998): Mesoscale eddies and the Kuroshio current observed by TOPEX/POSEIDON altimeteric data, JAMSTECR, **33**, 135-141 (in Japanese with English abstract).

Received December 12, 2003
Accepted June 15, 2004